



Effects of Heat Source/ Sink and non uniform temperature gradients on Darcian-Bènard-Magneto-Marangoni convection in composite layer horizontally enclosed by adiabatic boundaries

R. Sumithra¹ and N. Manjunatha^{2*}

Abstract

The problem of Bènard-Magneto-Marangoni convection in a composite layer which is horizontally infinite, is investigated for the Darcian case in the presence of constant heat source/sink in both the layers. This composite layer is enclosed by adiabatic boundaries and subjected to linear, parabolic and inverted parabolic temperature gradients. The eigenvalue, thermal Marangoni number is obtained in the closed form for lower rigid and upper free with surface tension velocity boundary combinations. The influence of various parameters on the eigenvalue against depth ratio is discussed. It is observed that the effect of heat source/sink is dominant in the fluid layer. The parameters which manipulate (advance or delay) the convection are determined.

Keywords

Heat source (sink), Marangoni convection, Magnetic field, Composite layer, Adiabatic boundaries.

AMS Subject Classification: 76-XX,76Rxx,76Sxx.

¹ Department of UG, PG Studies & Research in Mathematics, Government Science College Autonomous, Bengaluru, Karnataka, India;

² School of Applied Sciences, REVA University, Bengaluru, Karnataka, India.

*Corresponding author: ¹sumitra.diya@yahoo.com, ² manjunatha.n@reva.edu.in

Article History: Received 10 November 2019; Accepted 09 March 2020

©2020 MJM.

Contents

1	Introduction	373
2	Formulation of the problem	374
3	Boundary Conditions	376
4	Method of Solution	376
4.1	Linear temperature profile	376
4.2	Parabolic temperature profile	377
4.3	Inverted Parabolic temperature profile	377
5	Results and Discussion	378
6	Conclusion	381
	References	381

1. Introduction

The study of MHD flow is very important because of its applications in geophysics, astrophysics, engineering and

technology. The study of effect of magnetic field on temperature distribution with heat source/sink when fluid is capable of emitting and absorbing thermal radiations is of great importance in concerned with space applications and higher operating temperatures. The study of heat generation or absorption in moving fluids is important in several physical problems such as fluids undergoing exothermic or endothermic chemical reactions. The effect of heat source/sink in thermal convection is considered where there are high temperature differences between surfaces such as space craft bodies. The present model has applications in geophysics, astrophysics, aerospace, solar energy collection systems and also in the design of high operating temperature chemical process systems. The study of heat source/sink effects on heat transfer is very important because their effects are crucial in controlling the heat transfer also used as an effective parameter to control convection. The natural convection process in the presence of heat source/sink is presented in various physical

phenomena such as fire engineering, combustion modeling, nuclear energy, heat ex-changers, petroleum reservoir, etc. Internal heat source (sink) may arise due to heat released during chemical reactions in the fluid, radioactive decay, Ohmic heating by current in conductive liquid, produced by radiation from external medium there by helping in advancing or delaying convection. The several studies have been made on the single layer, Suneetha et al. [13] studied the thermal radiation effects on MHD flow past an impulsively started vertical plate in the presence of heat source/sink is investigated using implicit finite difference method of Crank-Nicholson type. Balasubrahmanyam *et al.* [1] studied the Soret effect on mixed convective heat and mass transfer through a porous medium confined in a cylindrical annulus under a radial magnetic field in the presence of a constant heat source/sink. Sudhakar Reddy *et al.* [9] studied the unsteady free convection unsteady flow of a viscous incompressible, electrically conducting, rotating liquid in a porous medium past an infinite isothermal vertical plate with constant heat source / sink in the presence of a uniform magnetic field applied perpendicular to the flow region. Thommaandru Ranga Rao *et al.* [15] investigates theoretically the problem of free convection boundary layer flow of nanofluids over a nonlinear stretching sheet in the presence of MHD and heat source/sink using fourth order Runge-Kutta method along with shooting technique. Dileep Kumar and Singh [2] investigated the effects of induced magnetic field and heat source/sink on fully developed laminar natural convective flow of a viscous incompressible and electrically conducting fluid in the presence of radial magnetic field by considering induced magnetic field into account. The governing equations of the considered model are transformed into simultaneously ordinary differential equations and solved analytically. Sudhakar Reddy *et al.* [10] studied the upshots of an unsteady MHD radiating nanofluid past a stretching sheet taking into account the heat source/sink using Runge-Kutta scheme along with shooting technique. Tasawar Hayat *et al.* [14] studied the heat source/sink in a magneto-hydrodynamic non-newtonian fluid flow in a porous medium.

Recently, Using Laplace transformation technique, the effect of heat source or sink past an impulsively started vertical plate under the influence of transverse magnetic field has been investigated by Garg and Shipra [3]. Garg and Shipra [4] investigated the heat source/sink effect on free convective incompressible viscous fluid flow and mass transfer in presence of uniform magnetic field applied normal to the infinite vertical plate moving with time dependent velocity by Laplace transformation method. The effect of heat source/sink on unsteady free-convective flow past an accelerated infinite vertical plate with mass diffusion in the presence of transverse magnetic field is investigated by Garg and Shipra [5]. They used the Laplace transformation technique to find the exact solution of the problem. Shipra and Garg [8] studied the effects of heat source/sink and chemical reaction with mass diffusion on free convective incompressible viscous fluid flow past an accelerated vertical plate with magnetic field has been inves-

tigated. Laplace transformation method has been applied to solve the system of linear partial differential equations. Lalrinpuia Tlau and Surender Ontela [6] investigated the generation of entropy in the presence of a heat source/sink in a sloping channel filled with porous medium in magnetohydrodynamic nanofluid flow using Homotopy analysis method. Naveen Dwivedi and Singh [7] studied the fully developed laminar magnetohydrodynamic free convection between two concentric vertical cylinders with Hall currents and heat source/sink, in the presence of the radial magnetic field. They found that the Hall current has a strong and direct impact on the flow character, such that the influence of the Hall parameter enhances the velocity fields in the appearance of heat source and sink.

For the composite layers, Sumithra and Manjunatha [11, 12] considered the effect of non-uniform temperature gradients on single and double diffusive magneto-Marangoni convection in a two layer system. They obtained the closed form of solution for Marangoni number.

So far no attempt has been made to analyze the effects in a composite layer with constant heat source/sink and uniform and non-uniform temperature gradients in the presence of a magnetic field and hence the present work is focused on this. In the present paper an attempt is made to study the effect of non-uniform temperature gradients on Bènard-Magneto-Marangoni convection in a composite layer in the presence of constant heat source (sink) in both the layers.

2. Formulation of the problem

Consider a horizontal single component, electrically conducting fluid saturated isotropic densely packed porous layer of thickness d_m underlying a single component fluid layer of thickness d with an imposed magnetic field intensity H_0 in the vertical z -direction and with heat sources Φ and Φ_m respectively. The lower surface of the porous layer rigid and the upper surface of the fluid layer is free with surface tension effects depending on temperature. A Cartesian coordinate system is chosen with the origin at the interface between porous and fluid layers and the z -axis, vertically upwards. The basic equations for fluid and porous layer respectively governing such a system are,

$$\nabla \cdot \vec{q} = 0 \quad (2.1)$$

$$\nabla \cdot \vec{H} = 0 \quad (2.2)$$

$$\rho_0 \left[\frac{\partial \vec{q}}{\partial t} + (\vec{q} \cdot \nabla) \vec{q} \right] = -\nabla P + \mu \nabla^2 \vec{q} + \mu_p (\vec{H} \cdot \nabla) \vec{H} \quad (2.3)$$

$$\frac{\partial T}{\partial t} + (\vec{q} \cdot \nabla) T = \kappa \nabla^2 T + \Phi \quad (2.4)$$

$$\frac{\partial \vec{H}}{\partial t} = \nabla \times \vec{q} \times \vec{H} + \nu_m \nabla^2 \vec{H} \quad (2.5)$$



$$\nabla_m \cdot \vec{q}_m = 0 \quad (2.6)$$

$$\nabla_m \cdot \vec{H} = 0 \quad (2.7)$$

$$\rho_0 \left[\frac{1}{\varepsilon} \frac{\partial \vec{q}_m}{\partial t} + \frac{1}{\varepsilon^2} (\vec{q}_m \cdot \nabla_m) \vec{q}_m \right] = -\nabla_m P_m - \frac{\mu}{K} \vec{q}_m + \mu_p (\vec{H} \cdot \nabla_m) \vec{H} \quad (2.8)$$

$$A \frac{\partial T_m}{\partial t} + (\vec{q}_m \cdot \nabla_m) T_m = \kappa_m \nabla_m^2 T_m + \Phi_m \quad (2.9)$$

$$\varepsilon \frac{\partial \vec{H}}{\partial t} = \nabla_m \times \vec{q}_m \times \vec{H} + v_{em} \nabla_m^2 \vec{H} \quad (2.10)$$

Where For fluid layer \vec{q} is the velocity vector, ρ_0 is the fluid density, t is time, μ is fluid viscosity, $P = p + \frac{\mu_p H^2}{2}$ is the total pressure, \vec{H} is the magnetic field, T is temperature, constant heat source Φ , κ thermal diffusivity of the fluid, $v_m = \frac{1}{\mu_p \sigma}$ is the magnetic viscosity and μ_p is the magnetic permeability. For porous layer ε is the porosity, K permeability of the porous medium, $A = \frac{(\rho_0 C_p)_m}{(\rho_0 C_p)_f}$ ratio of heat capacities, C_p specific heat, κ_m thermal diffusivity, Φ_m is constant heat source, $v_{em} = \frac{v_m}{\varepsilon}$ is the effective magnetic viscosity and the subscripts 'm' and 'f' (in these equations) denotes the quantities in porous layer and fluid layer respectively.

The aim of this paper is to investigate the stability of infinitesimal perturbations superposed on the basic quiescent state. The basic state of the liquid being quiescent is described by

$$\left. \begin{aligned} \vec{q} = \vec{q}_b = 0, P = P_b(z), T = T_b(z), \vec{H} = H_0(z) \\ \vec{q}_m = \vec{q}_{mb}, P_m = P_{mb}(z_m), T_m = T_{mb}(z_m), \vec{H} = H_0(z_m) \end{aligned} \right\} (2.11)$$

The basic state temperatures of $T_b(z)$ and $T_{mb}(z_m)$ are obtained as

$$T_b(z) = \left. \begin{aligned} \frac{-\Phi z(z-d)}{2\kappa} + \frac{(T_u - T_0)h(z)}{d} + T_0 \\ \text{in } 0 \leq z \leq d \end{aligned} \right\} (2.12)$$

$$T_{mb}(z_m) = \left. \begin{aligned} \frac{-\Phi_m z_m(z_m + d_m)}{2\kappa_m} + \frac{(T_0 - T_l)h_m(z_m)}{d_m} + T_0 \\ \text{in } -d_m \leq z_m \leq 0 \end{aligned} \right\} (2.13)$$

where $T_0 = \frac{\kappa d_m T_u + \kappa_m d T_l}{\kappa d_m + \kappa_m d} + \frac{d d_m (\Phi_m d_m + \Phi d)}{2(\kappa d_m + \kappa_m d)}$ is the interface temperature and $h(z)$ and $h_m(z_m)$ are temperature gradients in fluid and porous layer respectively and subscript 'b' denote the basic state.

We superimpose infinitesimal disturbances on the basic state for fluid and porous layer respectively

$$\left. \begin{aligned} \vec{q} = \vec{q}_b + \vec{q}', P = P_b + P', \\ T = T_b(z) + \theta, \vec{H} = H_0(z) + \vec{H}' \end{aligned} \right\} (2.14)$$

$$\left. \begin{aligned} \vec{q}_m = \vec{q}_{mb} + \vec{q}_m', P_m = P_{mb} + P_m', \\ T_m = T_{mb}(z_m) + \theta_m, \vec{H} = H_0(z_m) + \vec{H}' \end{aligned} \right\} (2.15)$$

Where the prime indicates the perturbation. Introducing (2.11) into (2.1) - (2.10), operating curl twice and eliminate the pressure term from equations (2.3) and (2.8), the resulting equations then nondimensionalized.

The dimensionless equations are then subjected to normal mode analysis as follows

$$\begin{bmatrix} W \\ \theta \\ H \end{bmatrix} = \begin{bmatrix} W(z) \\ \theta(z) \\ H(z) \end{bmatrix} f(x, y) e^{nt} \quad (2.16)$$

$$\begin{bmatrix} W_m \\ \theta_m \\ H \end{bmatrix} = \begin{bmatrix} W_m(z_m) \\ \theta_m(z_m) \\ H(z_m) \end{bmatrix} f_m(x_m, y_m) e^{n_m t} \quad (2.17)$$

with $\nabla^2 f + a^2 f = 0$ and $\nabla_{2m}^2 f_m + a_m^2 f_m = 0$, where a and a_m are the wave numbers, n and n_m are the frequencies, W and W_m are the dimensionless vertical velocities in fluid and porous layer respectively and obtain the following equations in $0 \leq z \leq 1$

$$\begin{aligned} (D^2 - a^2 + \frac{n}{Pr})(D^2 - a^2)W \\ = -Q\tau_{fm}D(D^2 - a^2)H \end{aligned} \quad (2.18)$$

$$(D^2 - a^2 + n)\theta + [h(z) + R_I^*(2z - 1)]W = 0 \quad (2.19)$$

$$(\tau_{fm}(D^2 - a^2) + n)H + DW = 0 \quad (2.20)$$

in $-1 \leq z_m \leq 0$

$$\begin{aligned} (1 - \frac{\beta^2 n_m}{Pr_m})(D_m^2 - a_m^2)W_m \\ = Q_m \tau_{mm} \beta^2 D_m (D_m^2 - a_m^2)H_m \end{aligned} \quad (2.21)$$

$$\begin{aligned} (D_m^2 - a_m^2 + An_m)\theta_m + [h_m(z_m) \\ + R_{Im}^*(2z_m + 1)]W_m = 0 \end{aligned} \quad (2.22)$$

$$\tau_{mm}(D_m^2 - a_m^2 + n_m \varepsilon)H_m + D_m W_m = 0 \quad (2.23)$$

where for fluid layer, $Pr = \frac{v}{\kappa}$ is the prandtl number, $Q = \frac{\mu_p H_0^2 d^2}{\mu \kappa \tau_{fm}}$ is the Chandrasekhar number, $\tau_{fm} = \frac{v_{mv}}{\kappa}$ is the diffusivity ratio.

For porous layer, $Pr_m = \frac{\varepsilon v_m}{\kappa_m}$ is the prandtl number, $Q_m = \frac{\mu_p H_0^2 d_m^2}{\mu \kappa_m \tau_{mm}} = Q \varepsilon \hat{d}^2$ is the Chandrasekhar number, $\tau_{mm} = \frac{v_{em}}{\kappa_m}$ is the diffusivity ratio. $R_I^* = \frac{R_I}{2(T_0 - T_u)}$,

$R_{Im}^* = \frac{R_{Im}}{2(T_l - T_0)}$, here R_I is the internal Rayleigh number for fluid layer and R_{Im} is the internal Rayleigh number for porous layer. $h(z)$ and $h_m(z_m)$ are the non-dimensional temperature gradients with $\int_0^1 h(z) dz = 1$ and $\int_0^1 h_m(z_m) dz_m = 1$, θ and θ_m are the temperature in fluid and porous layers respectively,

substituting the equation (2.20) in (2.18) and (2.23) in (2.21) and assume that the present problem satisfies the principle of



exchange of instability, so putting $n = n_m = 0$. We get, in $0 \leq z \leq 1$

$$(D^2 - a^2)^2 W = QD^2 W \quad (2.24)$$

$$(D^2 - a^2)\theta + [h(z) + R_I^*(2z - 1)]W = 0 \quad (2.25)$$

in $-1 \leq z_m \leq 0$

$$(D_m^2 - a_m^2)W_m = -Q_m\beta^2 D_m^2 W_m \quad (2.26)$$

$$(D_m^2 - a_m^2)\theta_m + [h_m(z_m) + R_{Im}^*(2z_m + 1)]W_m = 0 \quad (2.27)$$

3. Boundary Conditions

The boundary conditions are nondimensionalized and then subjected to normal mode expansion and are

$$\begin{aligned} D^2 W(1) + Ma^2 \theta(1) &= 0, \\ W(1) = 0, W_m(-1) = 0, \hat{T}W(0) &= W_m(0), \\ \hat{T}dDW(0) &= D_m W_m(0), \\ \hat{T}d^3\beta^2(D^3 W(0) - 3a^2 DW(0)) &= -D_m W_m(0), \\ D\theta(1) = 0, \theta(0) &= \hat{T}\theta_m(0), \\ D\theta(0) = D_m\theta_m(0), D_m\theta_m(-1) &= 0 \end{aligned} \quad (3.1)$$

where $\hat{T} = \frac{T_l - T_0}{T_0 - T_u}$ is the thermal ratio, $M = -\frac{\partial \sigma_t (T_0 - T_u)d}{\partial T \mu \kappa}$ is the thermal Marangoni number, $\beta = \sqrt{\frac{K}{d_m^2}}$ is the porous parameter and $\hat{d} = \frac{d_m}{d}$ is the depth ratio.

4. Method of Solution

The solutions W and W_m are obtained by solving (2.24) and (2.26) using the boundary conditions (3.1)

$$W(z) = A_1 [\cosh \delta z + a_1 \sinh \delta z + a_2 \cosh \zeta z + a_3 \sinh \zeta z] \quad (4.1)$$

$$W_m(z_m) = A_1 [a_4 \cosh \delta_m z_m + a_5 \sinh \delta_m z_m] \quad (4.2)$$

where

$$\begin{aligned} \delta &= \frac{\sqrt{Q} - \sqrt{Q + 4a^2}}{2}, \zeta = \frac{\sqrt{Q} + \sqrt{Q + 4a^2}}{2}, \\ \delta_m &= \sqrt{\frac{a_m^2}{1 + Q_m\beta^2}}, a_1 = -\frac{\Delta_2 a_3}{\Delta_1}, a_2 = \frac{\Delta_5 \Delta_7 - \Delta_8 \Delta_4}{\Delta_3 \Delta_7 - \Delta_6 \Delta_4}, \\ a_3 &= \frac{\Delta_5 \Delta_6 - \Delta_8 \Delta_3}{\Delta_4 \Delta_6 - \Delta_7 \Delta_3}, a_4 = \hat{T}(1 + a_2), a_5 = \frac{1}{\delta_m} (\hat{T} \hat{d} a_1 \delta + a_3 \zeta) \\ \Delta_1 &= \hat{d}^2 \beta^2 (\delta^3 - 3a^2 \delta) + \delta, \Delta_2 = \hat{d}^2 \beta^2 (\zeta^3 - 3a^2 \zeta) + \zeta, \\ \Delta_3 &= \hat{T} \cosh \delta_m, \Delta_4 = -\frac{\hat{d} \hat{T} \sinh \delta_m}{\delta_m} (\zeta - \frac{\Delta_2 \delta}{\Delta_1}), \\ \Delta_5 &= -\Delta_3, \Delta_6 = \cosh \zeta, \\ \Delta_7 &= \sinh \zeta - (\frac{\Delta_2}{\Delta_1}) \sinh \delta, \Delta_8 = -\cosh \delta \end{aligned}$$

4.1 Linear temperature profile

Consider the linear temperature profile of the form

$$h(z) = 1 \quad \text{and} \quad h_m(z_m) = 1 \quad (4.3)$$

Substituting equation (4.3) into (2.25) and (2.27), the temperature distributions θ and θ_m are obtained using the temperature boundary conditions, as follows

$$\theta(z) = A_1 [c_1 \cosh az + c_2 \sinh az + g_1(z)] \quad (4.4)$$

$$\theta_m(z_m) = A_1 [c_3 \cosh a_m z_m + c_4 \sinh a_m z_m + g_{m1}(z_m)] \quad (4.5)$$

where

$$g_1(z) = A_1 [\delta_1 - \delta_2 + \delta_3 - \delta_4], g_{m1}(z_m) = A_1 [\delta_5 - \delta_6]$$

$$\delta_1 = \frac{(E_2 z + E_1)}{(\delta^2 - a^2)} (\cosh \delta z + a_1 \sinh \delta z)$$

$$\delta_2 = \frac{2\delta E_2}{(\delta^2 - a^2)^2} (a_1 \cosh \delta z + \sinh \delta z)$$

$$\delta_3 = \frac{(E_2 z + E_1)}{(\zeta^2 - a^2)} (a_2 \cosh \zeta z + a_3 \sinh \zeta z)$$

$$\delta_4 = \frac{2\zeta E_2}{(\zeta^2 - a^2)^2} (a_3 \cosh \zeta z + a_2 \sinh \zeta z)$$

$$\delta_5 = \frac{(E_{1m} + E_{2m} z_m)}{(\delta_m^2 - a_m^2)} (a_4 \cosh \delta_m z_m + a_5 \sinh \delta_m z_m)$$

$$\delta_6 = \frac{2E_{2m} \delta_m}{(\delta_m^2 - a_m^2)^2} (a_5 \cosh \delta_m z_m + a_4 \sinh \delta_m z_m)$$

$$E_1 = R_I^* - 1, E_2 = -2R_I^*, E_{1m} = -(R_{Im}^* + 1),$$

$$E_{2m} = -2R_{Im}^*, c_1 = c_3 \hat{T} + \Delta_{10} - \Delta_{11},$$

$$c_2 = \frac{1}{a} (c_4 a_m + \Delta_{12} - \Delta_{13}),$$

$$c_3 = \frac{\Delta_{16} \Delta_{18} - \Delta_{19} \Delta_{14}}{-\Delta_{15} \Delta_{18} - \Delta_{17} \Delta_{14}}, c_4 = \frac{\Delta_{16} \Delta_{17} + \Delta_{19} \Delta_{15}}{\Delta_{14} \Delta_{17} + \Delta_{18} \Delta_{15}},$$

$$\Delta_9 = -[\delta_7 + \delta_8 + \delta_9 + \delta_{10}],$$

$$\delta_7 = \frac{\delta(E_2 + E_1)}{(\delta^2 - a^2)} (a_1 \cosh \delta + \sinh \delta),$$

$$\delta_8 = [\frac{E_2}{(\delta^2 - a^2)} - \frac{2\delta^2 E_2}{(\delta^2 - a^2)^2}] (\cosh \delta + a_1 \sinh \delta),$$

$$\delta_9 = \frac{\zeta(E_2 + E_1)}{(\zeta^2 - a^2)} (a_3 \cosh \zeta + a_2 \sinh \zeta),$$

$$\delta_{10} = [\frac{E_2}{(\zeta^2 - a^2)} - \frac{2\zeta^2 E_2}{(\zeta^2 - a^2)^2}] (a_2 \cosh \zeta + a_3 \sinh \zeta),$$

$$\Delta_{10} = \hat{T} [\frac{E_{1m} a_4}{(\delta_m^2 - a_m^2)} - \frac{2E_{2m} \delta_m a_5}{(\delta_m^2 - a_m^2)^2}]$$

$$\Delta_{11} = \frac{E_1}{(\delta^2 - a^2)} - \frac{2\delta a_1 E_2}{(\delta^2 - a^2)^2} + \Delta_{110}$$

$$\Delta_{110} = \frac{a_2 E_1}{(\zeta^2 - a^2)} - \frac{2\zeta a_3 E_2}{(\zeta^2 - a^2)^2}$$

$$\Delta_{12} = [\frac{E_{2m}}{(\delta_m^2 - a_m^2)} - \frac{2\delta_m^2 E_{2m}}{(\delta_m^2 - a_m^2)^2}] a_4 + \frac{a_5 E_{1m}}{(\delta_m^2 - a_m^2)}$$

$$\Delta_{13} = \frac{E_1 \delta a_1 + E_2}{(\delta^2 - a^2)} - \frac{2E_2 \delta^2}{(\delta^2 - a^2)^2} + \Delta_{130}$$

$$\Delta_{130} = \frac{E_1 \zeta a_3 + E_2 a_2}{(\zeta^2 - a^2)} - \frac{2a_2 E_2 \zeta^2}{(\zeta^2 - a^2)^2},$$

$$\Delta_{14} = a_m \cosh a_m, \Delta_{15} = a_m \sinh a_m,$$

$$\Delta_{16} = [\frac{-E_{2m}}{(\delta_m^2 - a_m^2)} + \frac{2\delta_m^2 E_{2m}}{(\delta_m^2 - a_m^2)^2}] \Delta_{160} - \Delta_{161},$$

$$\Delta_{160} = (a_4 \cosh \delta_m - a_5 \sinh \delta_m),$$

$$\Delta_{161} = \frac{\delta_m (E_{1m} - E_{2m})}{(\delta_m^2 - a_m^2)} (a_5 \cosh \delta_m - a_4 \sinh \delta_m),$$

$$\Delta_{17} = \hat{T} a \sinh a, \Delta_{18} = a_m \cosh a,$$

$$\Delta_{19} = \Delta_9 - a(\Delta_{10} - \Delta_{11}) \sinh a - (\Delta_{12} - \Delta_{13}) \cosh a$$



From the boundary condition (3.1), we have

$$M = \frac{-D^2W(1)}{a^2\theta(1)}$$

The thermal Marangoni number for the linear temperature profile is as follows

$$M_1 = \frac{-\Lambda_1}{a^2(c_1 \cosh a + c_2 \sinh a + \Lambda_2 + \Lambda_3)} \quad (4.6)$$

where

$$\Lambda_1 = \delta^2(\cosh \delta + a_1 \sinh \delta) + \zeta^2(a_2 \cosh \zeta + a_3 \sinh \zeta)$$

$$\Lambda_2 = \frac{(E_2 + E_1)}{(\delta^2 - a^2)}(\cosh \delta + a_1 \sinh \delta) - \Delta_{42}$$

$$\Delta_{42} = \frac{2\delta E_2}{(\delta^2 - a^2)^2}(a_1 \cosh \delta + \sinh \delta)$$

$$\Lambda_3 = \frac{(E_2 + E_1)}{(\zeta^2 - a^2)}(a_2 \cosh \zeta + a_3 \sinh \zeta) - \Delta_{43}$$

$$\Delta_{43} = \frac{2\zeta E_2}{(\zeta^2 - a^2)^2}(a_3 \cosh \zeta + a_2 \sinh \zeta)$$

4.2 Parabolic temperature profile

Consider the Parabolic temperature profile of the form

$$h(z) = 2z \quad \text{and} \quad h_m(z_m) = 2z_m \quad (4.7)$$

Substituting (4.7) into (2.25) and (2.27), the temperature distributions θ and θ_m are obtained using the temperature boundary conditions is as follows

$$\theta(z) = A_1[c_5 \cosh az + c_6 \sinh az + g_2(z)] \quad (4.8)$$

$$\theta_m(z_m) = A_1[c_7 \cosh a_m z_m + c_8 \sinh a_m z_m + g_{m2}(z_m)] \quad (4.9)$$

where

$$g_2(z) = A_1[\delta_{11} - \delta_{12} + \delta_{13} - \delta_{14}], g_{m2}(z_m) = A_1[\delta_{15} - \delta_{16}]$$

$$\delta_{11} = \frac{(E_4 z + E_3)}{(\delta^2 - a^2)}(\cosh \delta z + a_1 \sinh \delta z)$$

$$\delta_{12} = \frac{2\delta E_4}{(\delta^2 - a^2)^2}(a_1 \cosh \delta z + \sinh \delta z)$$

$$\delta_{13} = \frac{(E_4 z + E_3)}{(\zeta^2 - a^2)}(a_2 \cosh \zeta z + a_3 \sinh \zeta z)$$

$$\delta_{14} = \frac{2\zeta E_4}{(\zeta^2 - a^2)^2}(a_3 \cosh \zeta z + a_2 \sinh \zeta z)$$

$$\delta_{15} = \frac{(E_{3m} + E_{4m} z_m)}{(\delta_m^2 - a_m^2)}(a_4 \cosh \delta_m z_m + a_5 \sinh \delta_m z_m)$$

$$\delta_{16} = \frac{2E_{4m} \delta_m}{(\delta_m^2 - a_m^2)^2}(a_5 \cosh \delta_m z_m + a_4 \sinh \delta_m z_m),$$

$$E_3 = R_I^*, E_4 = -2(R_I^* + 1),$$

$$E_{3m} = -R_{Im}^*, E_{4m} = -2(R_{Im}^* + 1)$$

$$c_5 = c_7 \hat{T} + \Delta_{21} - \Delta_{22}, c_6 = \frac{1}{a}(c_8 a_m + \Delta_{23} - \Delta_{24}),$$

$$c_7 = \frac{\Delta_{30} \Delta_{25} - \Delta_{27} \Delta_{29}}{\Delta_{28} \Delta_{25} + \Delta_{26} \Delta_{29}}, c_8 = \frac{\Delta_{30} \Delta_{26} + \Delta_{27} \Delta_{28}}{\Delta_{29} \Delta_{26} + \Delta_{25} \Delta_{28}},$$

$$\Delta_{20} = -[\delta_{17} + \delta_{18} + \delta_{19} + \delta_{20}],$$

$$\delta_{17} = \frac{\delta(E_4 + E_3)}{(\delta^2 - a^2)}(a_1 \cosh \delta + \sinh \delta),$$

$$\delta_{18} = \left[\frac{E_4}{(\delta^2 - a^2)} - \frac{2\delta^2 E_4}{(\delta^2 - a^2)^2} \right] (\cosh \delta + a_1 \sinh \delta),$$

$$\delta_{19} = \frac{\zeta(E_4 + E_3)}{(\zeta^2 - a^2)}(a_3 \cosh \zeta + a_2 \sinh \zeta),$$

$$\delta_{20} = \left[\frac{E_4}{(\zeta^2 - a^2)} - \frac{2\zeta^2 E_4}{(\zeta^2 - a^2)^2} \right] (a_2 \cosh \zeta + a_3 \sinh \zeta),$$

$$\Delta_{21} = \hat{T} \left[\frac{E_{3m} a_4}{(\delta_m^2 - a_m^2)} - \frac{2E_{4m} \delta_m a_5}{(\delta_m^2 - a_m^2)^2} \right],$$

$$\Delta_{22} = \frac{E_3}{(\delta^2 - a^2)} - \frac{2\delta a_1 E_4}{(\delta^2 - a^2)^2} + \Delta_{220}$$

$$\Delta_{220} = \frac{a_2 E_3}{(\zeta^2 - a^2)} - \frac{2\zeta a_3 E_4}{(\zeta^2 - a^2)^2},$$

$$\Delta_{23} = \left[\frac{E_{4m}}{(\delta_m^2 - a_m^2)} - \frac{2\delta_m^2 E_{4m}}{(\delta_m^2 - a_m^2)^2} \right] a_4 + \frac{a_5 E_{3m}}{(\delta_m^2 - a_m^2)}$$

$$\Delta_{24} = \frac{E_3 \delta a_1 + E_4}{(\delta^2 - a^2)} - \frac{2E_4 \delta^2}{(\delta^2 - a^2)^2} + \Delta_{240}$$

$$\Delta_{240} = \frac{E_3 \zeta a_3 + E_4 a_2}{(\zeta^2 - a^2)} - \frac{2a_2 E_4 \zeta^2}{(\zeta^2 - a^2)^2},$$

$$\Delta_{25} = a_m \cosh a_m, \Delta_{26} = a_m \sinh a_m,$$

$$\Delta_{27} = - \left[\frac{E_{4m}}{(\delta_m^2 - a_m^2)} - \frac{2\delta_m^2 E_{4m}}{(\delta_m^2 - a_m^2)^2} \right] \Delta_{160} - \Delta_{270}$$

$$\Delta_{270} = \frac{\delta_m(E_{3m} - E_{4m})}{(\delta_m^2 - a_m^2)}(a_5 \cosh \delta_m - a_4 \sinh \delta_m),$$

$$\Delta_{28} = a \hat{T} \sinh a, \Delta_{29} = a_m \cosh a,$$

$$\Delta_{30} = \Delta_{20} - a(\Delta_{21} - \Delta_{22}) \sinh a - (\Delta_{23} - \Delta_{24}) \cosh a$$

From the boundary condition (3.1), the thermal Marangoni number for parabolic temperature profile is as follows

$$M_2 = \frac{-\Lambda_1}{a^2(c_5 \cosh a + c_6 \sinh a + \Lambda_4 + \Lambda_5)} \quad (4.10)$$

where

$$\Lambda_4 = \frac{(E_4 + E_3)}{(\delta^2 - a^2)}(\cosh \delta + a_1 \sinh \delta) - \Delta_{44}$$

$$\Delta_{44} = \frac{2\delta E_4}{(\delta^2 - a^2)^2}(a_1 \cosh \delta + \sinh \delta)$$

$$\Lambda_5 = \frac{(E_4 + E_3)}{(\zeta^2 - a^2)}(a_2 \cosh \zeta + a_3 \sinh \zeta) - \Delta_{45}$$

$$\Delta_{45} = \frac{2\zeta E_4}{(\zeta^2 - a^2)^2}(a_3 \cosh \zeta + a_2 \sinh \zeta)$$

4.3 Inverted Parabolic temperature profile

Consider the inverted Parabolic temperature profile of the form

$$h(z) = 2(1 - z) \quad \text{and} \quad h_m(z_m) = 2(1 - z_m) \quad (4.11)$$

Substituting (4.11) into (2.25) and (2.27), the temperature distributions θ and θ_m are obtained using the temperature boundary conditions, as follows

$$\theta(z) = A_1[c_9 \cosh az + c_{10} \sinh az + g_3(z)] \quad (4.12)$$

$$\theta_m(z_m) = A_1[c_{11} \cosh a_m z_m + c_{12} \sinh a_m z_m + g_{m3}(z_m)] \quad (4.13)$$

where

$$g_3(z) = A_1[\delta_{21} - \delta_{22} + \delta_{23} - \delta_{24}], g_{m3}(z_m) = A_1[\delta_{25} - \delta_{26}]$$

$$\delta_{21} = \frac{(E_6 z + E_5)}{(\delta^2 - a^2)}(\cosh \delta z + a_1 \sinh \delta z)$$



$$\begin{aligned} \delta_{22} &= \frac{2\delta E_6}{(\delta^2 - a^2)^2} (a_1 \cosh \delta z + \sinh \delta z) \\ \delta_{23} &= \frac{(E_6 z + E_5)}{(\zeta^2 - a^2)} (a_2 \cosh \zeta z + a_3 \sinh \zeta z) \\ \delta_{24} &= \frac{2\zeta E_6}{(\zeta^2 - a^2)^2} (a_3 \cosh \zeta z + a_2 \sinh \zeta z) \\ \delta_{25} &= \frac{(E_{5m} + E_{6m} z_m)}{(\delta_m^2 - a_m^2)} (a_4 \cosh \delta_m z_m + a_5 \sinh \delta_m z_m) \\ \delta_{26} &= \frac{2E_{6m} \delta_m}{(\delta_m^2 - a_m^2)^2} (a_5 \cosh \delta_m z_m + a_4 \sinh \delta_m z_m), \\ E_5 &= R_I^* - 2, E_6 = 2(1 - R_I^*), \\ E_{5m} &= -2 - R_{Im}^*, E_{6m} = 2(1 - R_{Im}^*) \\ c_9 &= c_{11} \hat{T} + \Delta_{32} - \Delta_{33}, c_{10} = \frac{1}{a} (c_{12} a_m + \Delta_{34} - \Delta_{35}), \\ c_{11} &= \frac{\Delta_{36} \Delta_{41} - \Delta_{38} \Delta_{40}}{\Delta_{39} \Delta_{36} + \Delta_{37} \Delta_{40}}, c_{12} = \frac{\Delta_{41} \Delta_{37} + \Delta_{39} \Delta_{38}}{\Delta_{40} \Delta_{37} + \Delta_{36} \Delta_{39}}, \\ \Delta_{31} &= -[\delta_{27} + \delta_{28} + \delta_{29} + \delta_{30}], \\ \delta_{27} &= \frac{\delta(E_6 + E_5)}{(\delta^2 - a^2)} (a_1 \cosh \delta + \sinh \delta), \\ \delta_{28} &= \left[\frac{E_6}{(\delta^2 - a^2)} - \frac{2\delta^2 E_6}{(\delta^2 - a^2)^2} \right] (\cosh \delta + a_1 \sinh \delta), \\ \delta_{29} &= \frac{\zeta(E_6 + E_5)}{(\zeta^2 - a^2)} (a_3 \cosh \zeta + a_2 \sinh \zeta), \\ \delta_{30} &= \left[\frac{E_6}{(\zeta^2 - a^2)} - \frac{2\zeta^2 E_6}{(\zeta^2 - a^2)^2} \right] (a_2 \cosh \zeta + a_3 \sinh \zeta), \\ \Delta_{32} &= \hat{T} \left[\frac{E_{5m} a_4}{(\delta_m^2 - a_m^2)} - \frac{2E_{6m} \delta_m a_5}{(\delta_m^2 - a_m^2)^2} \right], \\ \Delta_{33} &= \frac{E_5}{(\delta^2 - a^2)} - \frac{2\delta a_1 E_6}{(\delta^2 - a^2)^2} + \frac{a_2 E_5}{(\zeta^2 - a^2)} - \frac{2\zeta a_3 E_6}{(\zeta^2 - a^2)^2}, \\ \Delta_{34} &= \left[\frac{E_{6m}}{(\delta_m^2 - a_m^2)} - \frac{2\delta_m^2 E_{6m}}{(\delta_m^2 - a_m^2)^2} \right] a_4 + \frac{a_5 E_{5m}}{(\delta_m^2 - a_m^2)} \\ \Delta_{35} &= \frac{E_5 \delta a_1 + E_6}{(\delta^2 - a^2)} - \frac{2E_6 \delta^2}{(\delta^2 - a^2)^2} + \Delta_{350} \\ \Delta_{350} &= \frac{E_5 \zeta a_3 + E_6 a_2}{(\zeta^2 - a^2)} - \frac{2a_2 E_6 \zeta^2}{(\zeta^2 - a^2)^2}, \\ \Delta_{36} &= a_m \cosh a_m, \Delta_{37} = a_m \sinh a_m, \\ \Delta_{38} &= - \left[\frac{E_{6m}}{(\delta_m^2 - a_m^2)} - \frac{2\delta_m^2 E_{6m}}{(\delta_m^2 - a_m^2)^2} \right] \Delta_{160} - \Delta_{380} \\ \Delta_{380} &= \frac{\delta_m (E_{5m} - E_{6m})}{(\delta_m^2 - a_m^2)} (a_5 \cosh \delta_m - a_4 \sinh \delta_m), \\ \Delta_{39} &= a \hat{T} \sinh a, \Delta_{40} = a_m \cosh a, \\ \Delta_{41} &= \Delta_{31} - a(\Delta_{32} - \Delta_{33}) \sinh a - (\Delta_{34} - \Delta_{35}) \cosh a \end{aligned}$$

From the boundary condition (3.1), the thermal Marangoni number for inverted parabolic temperature profile is as follows

$$M_3 = \frac{-\Lambda_1}{a^2(c_9 \cosh a + c_{10} \sinh a + \Lambda_6 + \Lambda_7)} \quad (4.14)$$

where

$$\begin{aligned} \Lambda_6 &= \frac{(E_6 + E_5)}{(\delta^2 - a^2)} (\cosh \delta + a_1 \sinh \delta) - \Delta_{46} \\ \Delta_{46} &= \frac{2\delta E_6}{(\delta^2 - a^2)^2} (a_1 \cosh \delta + \sinh \delta) \\ \Lambda_7 &= \frac{(E_6 + E_5)}{(\zeta^2 - a^2)} (a_2 \cosh \zeta + a_3 \sinh \zeta) - \Delta_{47} \\ \Delta_{47} &= \frac{2\zeta E_6}{(\zeta^2 - a^2)^2} (a_3 \cosh \zeta + a_2 \sinh \zeta) \end{aligned}$$

5. Results and Discussion

The thermal Marangoni number M is obtained as an expression of the depth ratio \hat{d} , the horizontal wave numbers a and a_m both for the fluid and porous layers, the porous parameter β , the thermal ratio \hat{T} , R_I and R_{Im} the internal Rayleigh numbers for the fluid and porous layers and the Chandrasekhar number Q . This thermal Marangoni number M is drawn versus the depth ratio \hat{d} . From the graphs it is evident that, for smaller values of \hat{d} , the thermal Marangoni number M remains constant and then increases as the values of depth ratio is further increased. The effects of the horizontal wave number a , the porous parameter β , the Chandrasekhar number Q , R_I internal Rayleigh number and the thermal ratio \hat{T} on the thermal Marangoni are displayed in the following figures for other fixed parameters.

Fig.1 exhibits the effects of the horizontal wave number a on the values of thermal Marangoni number M for the fixed parameters $Q = 50, a = 1.0, \varepsilon = 1, \beta = 0.1, \hat{T} = 1.5, R_I = -3$ and $R_{Im} = 1$. The values of a are 0.9, 1.0 and 1.1. From the figure it is clear that for a fixed depth ratio, increase in the values of a , decreases the thermal Marangoni number. Hence the system becomes stable by decreasing the horizontal wave number. Similar effects are observed for all the three profiles, i.e., for linear, parabolic and inverted parabolic profiles.

Fig.2 depicts the effects of β , the porous parameter on the thermal Marangoni number and it is for $\beta = 0.1, 0.2$ and 0.3 . The curves are diverging, which indicates that the effect of the porous parameter is dominant for larger values of \hat{d} , i.e., the effect of porous parameter is prominent for the porous layer dominant systems and for a fixed values of \hat{d} , the increase in the value of β , shows the increase in the Marangoni number. Hence the system can be stabilized by increasing the value of β . Though there is more window for the fluid, the system still remains stabilized, this may be due to presence of magnetic field.

The effects of Chandrasekhar number Q is displayed in Fig.3 for the linear, parabolic and inverted parabolic temperature profiles. The values of Q taken are 50, 60 and 70. The curves are for all the three profiles are slightly diverging indicating the prominence of Q for larger depth ratio values i.e., for porous layer dominant system. For a fixed depth ratio, the increase in the value of Q increases the thermal Marangoni number, hence the Darcy- Bénard-Magneto-Marangoni convection can be advanced by decreasing the values of Q and hence the system can be destabilized.

The effect of internal Rayleigh number R_I on the Marangoni number is similar for all the three temperature profiles depicted the Fig. 4 for $R_I = -3, -4$ and -5 . Decreasing the values of R_I , the Marangoni number increases, hence the Darcy-Bénard-Magneto-Marangoni convection can be delayed by decreasing the values of R_I . Hence the heat absorption makes the system stable.



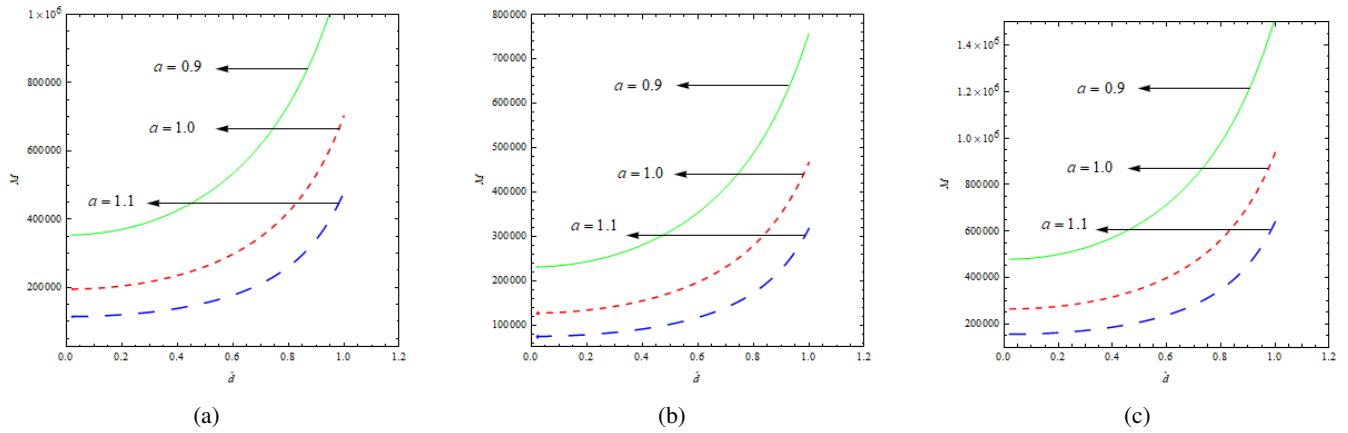


Figure 1. Effects of horizontal wavenumber α

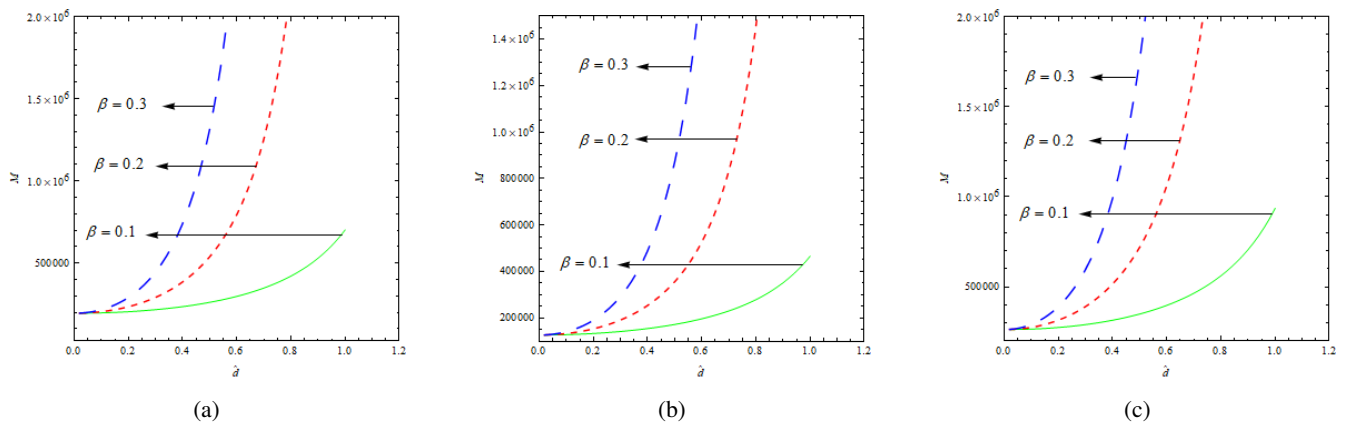


Figure 2. Effects of porous parameter β

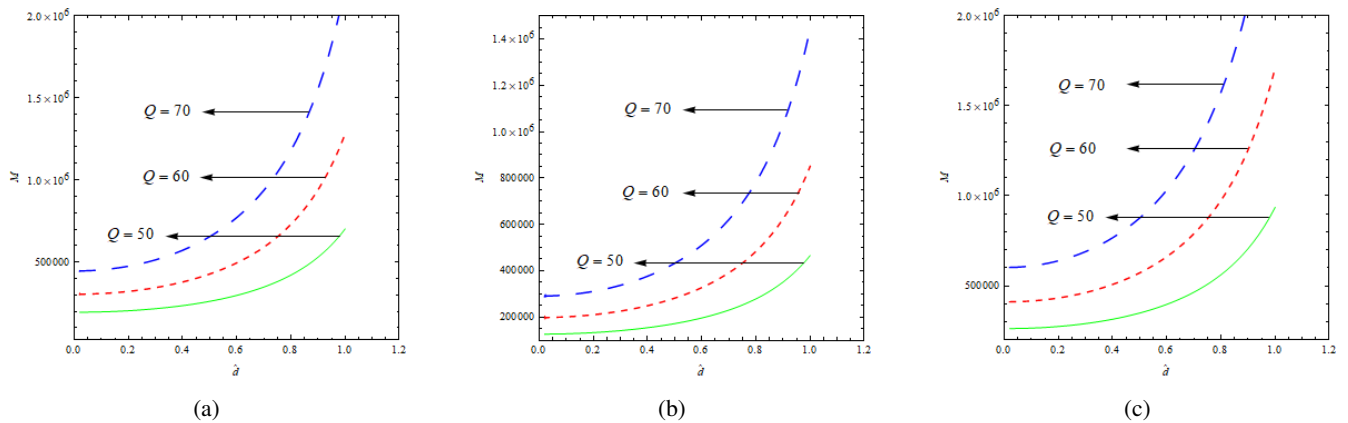


Figure 3. Effects of Chandrasekhar number Q



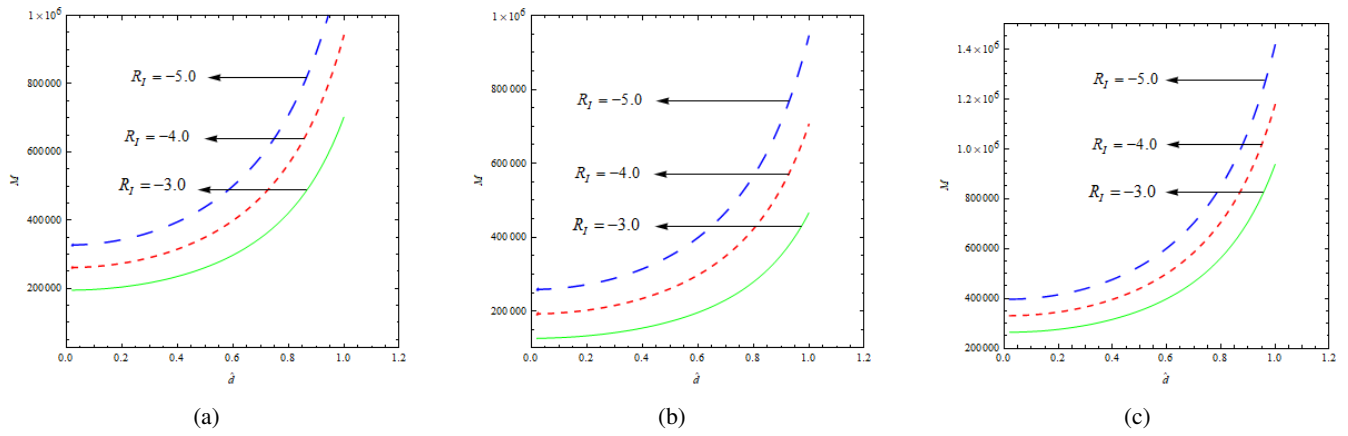


Figure 4. Effects of internal Rayleigh number R_I

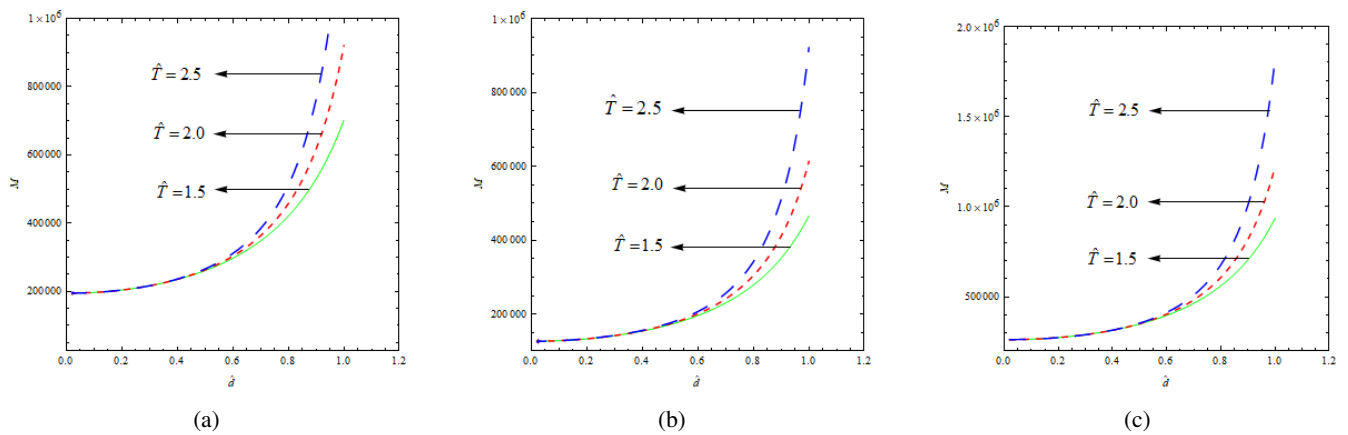


Figure 5. Effects of thermal ratio \hat{T}



The effects of thermal ratio \hat{T} on the thermal Marangoni number is shown in the Fig.5 for all three temperature profiles. The curves are diverging slightly for larger values of depth ratio, which indicates that the effect of \hat{T} is effective only for the larger values of \hat{d} and the increase in the value of \hat{T} increases the Marangoni number M hence, the system can be stabilized by decreasing the value of \hat{T} .

6. Conclusion

Following conclusions are drawn from this study

- By decreasing the values of horizontal wavenumber a and the internal Rayleigh numbers R_I , one can delay the Darcy-Benard-Magneto-Marangoni convection.
- By decreasing the values of porous parameter β , the Chandrasekhar number Q and the thermal ratio \hat{T} , one can advance Darcy-Benard-Magneto-Marangoni convection.
- There is no effect of internal Rayleigh number R_{Im} on the Darcy-Benard-Magneto-Marangoni convection.
- The parameters β , Q and \hat{T} play an important role for the porous layer dominant composite layer.
- The inverted parabolic temperature gradient is the highly stable of all the three gradients.
- The effects of the physical parameters is similar for all the three temperature gradients.

Acknowledgment

The authors are thankful to Late Prof. N. Rudraiah and Hon. Prof. I. S. Shivakumara, Professor, Department of Mathematics, Bangalore University, Bengaluru, for their help during the formulation of the problem.

References

- [1] M. Balasubrahmanyam, P. Sudarsan Reddy and R. Siva Prasad, Soret effect on mixed convective heat and mass transfer through a porous medium confined in a cylindrical annulus under a radial magnetic field in the presence of a constant heat source/sink, *Int. J. of Appl. Math and Mech.*, 7(8)(2011), 1–17.
- [2] Dileep Kumar and A.K. Singh, Effects of heat source/sink and induced magnetic field on natural convective flow in vertical concentric annuli, *Alexandria Engineering Journal*, 55(4)(2016), 3125–3133.
- [3] B. P. Garg and Shipra, Effect of heat source/sink on free connective MHD flow past an exponentially accelerated infinite plate with mass diffusion and chemical reaction, *Journal of Rajasthan Academy of Physical Sciences*, 17(3-4)(2018), 151–164.
- [4] B. P. Garg and Shipra, Exact solution of MHD free convective and mass transfer flow near a moving vertical plate in the presence of heat source/sink, *Journal of Rajasthan Academy of Physical Sciences*, 18 (1-2)(2019), 25–44.
- [5] B. P. Garg and Shipra, Effect of heat source/sink on unsteady free convective MHD flow past a linearly accelerated vertical plate with mass diffusion, *International Journal of Scientific Research and Reviews*, 8(2)(2019), 1437–1454.
- [6] Lalrinpuia Tlau and Surender Ontela, Entropy generation in MHD nanofluid flow with heat source/sink, *SN Applied Sciences*, 1(2019), 1672–1679.
- [7] Naveen Dwivedi and Ashok kumar Singh, Influence of Hall current on hydromagnetic natural convective flow between two vertical concentric cylinders in presence of heat source/sink, *Heat Transfer-Asian Res.*, (2020), 1–16.
- [8] Shipra and B. P. Garg, Effect of heat source/sink on free connective MHD flow past an exponentially accelerated infinite plate with mass diffusion and chemical reaction, *International Journal of Innovative Technology and Exploring Engineering*, 8(9S)(2019), 696–702.
- [9] T. Sudhakar Reddy, O. Siva Prasad Reddy, S. V. K. Varma and M. C. Raju, Heat transfer in hydro magnetic rotating flow of viscous fluid through a non-homogeneous porous medium with constant heat source/sink, *International Journal of Mathematical Archive*, 3(8)(2012), 2964–2973.
- [10] T.Sudhakara Reddy, N. Bhaskar Reddy, Pandikunta Sreenivasulu and T. Poornima, Magneto hydrodynamic convective flow of radiating nanofluid past a stretching surface in presence of heat source/sink, *Int. Journal of Applied Sciences and Engineering Research*, 5(4)(2016), 328–340.
- [11] R. Sumithra and N. Manjunatha, Analytical study of surface tension driven magneto convection in a composite layer bounded by adiabatic boundaries, *International Journal of Engineering and Innovative Technology*, 6 (1) (2012), 249–257.
- [12] R. Sumithra and N. Manjunatha, Effects of parabolic and inverted parabolic temperature gradients on magneto marangoni convection in a composite layer, *International Journal of Current Research*, 6(3)(2014), 5435–5450.
- [13] S. Suneetha, N. Bhaskar Reddy and V. Ramachandra Prasad, Radiation and mass transfer effects on MHD free convective dissipative fluid in the presence of heat source/sink, *Journal of Applied Fluid Mechanics*, 4(1)(2011), 107–113.
- [14] Tasawar Hayat, Muhammad Awais and Amna Imtiaz, Heat Source/Sink in a Magneto-Hydrodynamic Non-Newtonian Fluid Flow in a Porous Medium: Dual Solutions, *PLoS ONE*, 11(9)(2016), 1–16.
- [15] Thommaandru Ranga Rao, Kotha Gangadhar, B. Hema Sundar Raju and M. Venkata Subba Rao, Heat source/sink effects of heat and mass transfer of magneto-nanofluids



over a nonlinear stretching sheet, *Advances in Applied Science Research*, 5 (3)(2014), 114–129.

ISSN(P):2319 – 3786
Malaya Journal of Matematik
ISSN(O):2321 – 5666

